ADVANCED FUNCTIONAL MATERIALS

Supporting Information

for *Adv. Funct. Mater.*, DOI: 10.1002/adfm.202002560

Porous Silicon Nanoparticles Embedded in Poly(lactic-*co*-glycolic acid) Nanofiber Scaffolds Deliver Neurotrophic Payloads to Enhance Neuronal Growth

*Jonathan M. Zuidema, Courtney M. Dumont, Joanna Wang, Wyndham M. Batchelor, Yi-Sheng Lu, Jinyoung Kang, Alessandro Bertucci, Noel M. Ziebarth, Lonnie D. Shea, and Michael J. Sailor**

Supporting Information

Porous Silicon Nanoparticles Embedded in Poly(lactic-*co*-glycolic acid) Nanofiber Scaffolds Deliver Neurotrophic Payloads to Enhance Neuronal Growth

*Jonathan M. Zuidema, Courtney M. Dumont, Joanna Wang, Wyndham M. Batchelor, Yi-Sheng Lu, Jinyoung Kang, Alessandro Bertucci, Noel M. Ziebarth, Lonnie D. Shea, and Michael J. Sailor**

Experimental Section

Preparation of Porous Silicon Nanoparticles: The pSiNPs were prepared following the previously reported "perforation etching" procedure.[1] Highly boron-doped p-type silicon wafers (≈1 mΩ cm resistivity, 100 mm diameter, Virginia Semiconductor, Inc.) were anodized in an electrolyte composed of 3:1 (*v:v*) 48% aqueous HF:ethanol. CAUTION: HF is highly toxic and corrosive and contact with skin should be avoided. Procedures involving HF should always be carried out in a fume hood configured to handle HF and the operator should wear appropriate protective gloves, gown, and face shield. The etching waveform consisted of a square wave in which a lower current density of 46 mA cm^{-2} was applied for 1.818s, followed by a higher current density pulse of 365 mA cm^{-2} applied for 0.363 s. This waveform was repeated for 140 cycles, generating a stratified pSi film with thin, high porosity "perforations" repeating approximately every 180 nm through the porous layer. The film was removed from the silicon substrate by application of a current density of 3.4 mA cm^{-2} for 150 s in a solution containing 1:20 (*v:v*) of 48% aqueous HF:ethanol. The freestanding film was fractured into nanoparticles of mean diameter (z-average, intensity based dynamic light scattering measurement) 187 nm (Table S1) by immersion in DI H_2O (1 film/1 mL of DI water) and ultrasonication (1.9 L Ultrasonic Cleaner No. 97043, VWR, inc., 35 kHZ) for ≈ 18 h. This protocol generated pSiNPs with pore sizes between 10-20 nm,[2] verified by electron microscopy.

Preparation of bpV(HOpic)-Loaded Porous Silicon Nanoparticles: First, as-etched pSiNPs (1mg mL^{-1}) were suspended in a 0.1mM aqueous solution of sodium tetraborate and reacted for 90 min. at room temperature on a vortex mixer.[3] Prior work has shown that during the reaction, a passivating silicon oxide layer replaces the hydrogen-terminated pSi surface, resulting in a Si-SiO_2 core-shell type of structure that is photoluminescent. Following the reaction, the pSiNPs were centrifuged for 10 min. at 15,000 RPM (Eppendorf 5424R) and washed 2x with deionized water (DI H_2O), 1x with 100% ethanol, 1x with 50:50 ethanol:dichloromethane (DCM), and 1x 100% DCM. After the washing steps, ~1mg of pSiNPs were suspended in DCM (400 µL), an aliquot of 2,2-dimethoxy-1,6-diaza-2-silacyclooctane (Gelest) (100 µL) was added, and the mixture was agitated for 1 h to place a terminal amine on the particles.[4] The resulting particles were then washed 2x by centrifugation from DCM, 1x from 100% ethanol, and 1x from DI H_2O. 1 mg of amine-terminated pSiNPs were then suspended in 1 mL of an aqueous solution of 2.9 mM bpV(HOpic) (SML0884, Sigma Aldrich) and mixed *via* vortex for 1h. The pSiNPs were then washed 1X with DI H_2O. The amount of bpV(HOpic) loaded into the pSiNPs was calculated from the initial and final concentrations of the loading and washing solution (n=3) using the UV-vis absorbance at λ= 305nm.[5] The final mass loading was determined to be 16 ±0.6%, calculated as the mass of drug loaded divided by the total mass of the drug-loaded pSiNPs. For control cell culture experiments, empty amine-functionalized pSiNPs were used instead of the bpV(HOpic)-loaded pSiNPs.

Preparation of TrkB Aptamer-Loaded Porous Silicon Nanoparticles: A stock solution of 4 M calcium chloride ($CaCl_2$) (M_W = 110.98, anhydrous, Spectrum Chemicals) was prepared in DNase-free water. The solution was centrifuged to remove any precipitates. The RNA aptamer used is a 50-nt RNA sequence:[6]

(5'-GGGAGGACGAUGCGGUCGUAUUAUCCGCUGCACGCAGACGACUCGCCCGA-3') (Biosearch Technologies). The lyophilized TrkB Aptamer was re-suspended in DNase-free water at a concentration of 100 μM. 200 μL of the 100 μM DNA solution was added to a pSiNP solution (1 mg pSiNPs, 300 μL DNAse-free water). This solution was then mixed with 500 μL of 4 M $CaCl_2$, giving a final concentration of 20 μM TrkB Aptamer, 1 mg pSiNPs, and 2 M $CaCl_2$ in 1 mL of DNAse-free water. The solution was agitated for 60 min at room temperature, and then centrifuged for 10 min at 15,000 RPM. pSiNPs were washed 1x in DI H_2O, 1x in 50% ethanol:DI H_2O, and 1x in absolute ethanol. RNA-loading efficiency was determined by measuring the supernatants of each centrifugation step using a NanoDrop 2000 spectrometer (Thermo Science, ND-2000), and the aptamer loading[7] was determined to be 14 ± 0.3% of RNA by mass, calculated as the mass of RNA loaded divided by the total mass of the RNA-loaded pSiNPs. For control cell culture experiments, a 22-nt DNA sequence (5'-TCAACATCAGTCTGATAAGCTA-3') (Biosearch Technologies) was loaded with the same procedure described above.

Preparation of NGF-Loaded Porous Silicon Nanoparticles: Recombinant human beta-nerve growth factor (NGF) (256-GF, R&D Systems) was dissolved in 1x phosphate-buffered saline (PBS, Thermo Fisher Scientific) (pH = 7.4) that contained 0.5 mg mL^{-1} bovine serum albumin (BSA) (Sigma Aldrich) as a stabilizing agent at a concentration of 100 μg mL^{-1}. As-etched pSiNPs were suspended in this solution at a concentration of 1 mg mL^{-1} and then mixed on a rotating mixer for ~18 h at room temperature. The pSiNPs were centrifuged and washed 3 times with DI H_2O to remove surface adsorbed protein. The amount of NGF loaded into the pSiNPs was calculated from the initial and final concentrations of the loading and washing solution (n=3) using a Human beta-NGF DuoSet ELISA (DY256, R&D Systems) according to the manufacturers' protocol. The final mass loading (defined above) was found to be 0.213

± 0.07%. For control cell culture experiments, BSA-loaded pSiNPs were used instead of NGF-loaded pSiNPs.

Fabrication of PLGA and Hybrid pSiNP/PLGA Nanofibers: Nebulization fabrication of 75:25 poly(DL-lactide-*co*-glycolide) (B6007-1, LACTEL Absorbable Polymers) nanofibers was adapted from a previously published method.[8] In order to incorporate the various pSiNPs into the nanofiber scaffolds, pSiNPs were first washed 1 time with pure ethanol. The pSiNPs were then pelleted by centrifugation and re-suspended in chloroform. This solution was added to PLGA dissolved in chloroform, for a final concentration of 6% (*w/w*) PLGA. 0.1 mg bpV(HOpic)-pSiNPs were added to 500 mg of the 6% PLGA solution, 2 mg of TrkB aptamer-pSiNPs were added to 500 mg of 6% PLGA solution, and 2 mg of NGF-pSiNPs were added to 500 mg of 6% PLGA solution. The solution was added to the hopper of an airbrush (Model G222, Master Airbrush), and nebulized under nitrogen gas at 20 psi to generate fibers. To create aligned fibers, the airbrush nozzle was aimed downwards at a 20° angle. The collection surface was then aimed downward at a 10° angle. The nanofibers were collected onto PLGA films which had been cast onto 15x15 mm cover glass (Knittel Glass) slides. In order to ensure relatively equal nanofiber surface coverage, 10 seconds of nanofiber spray was used to deposit ~ 2mg of nanofibers onto each film. In previous work the percent by mass of silicon in this formulation was determined through inductively coupled plasma atomic emission spectrometry, and in that work it was verified that the experimentally determined mass percentage of silicon was within that calculated from the mass composition of the non-volatile starting materials to within 10%.[2] For this study, we used this calculated mass to report the total silicon content in the hybrid nanofibers.

Materials Characterization: Porosity of etched silicon was verified using the Spectroscopic Liquid Infiltration Method (SLIM) measurement.[9] TEM images were obtained with a JEOL-

1200 EX II 120 kV instrument. Scanning electron microscope (SEM) images and energy dispersive X-ray (EDX) analyses were obtained using a Zeiss Sigma 500 scanning electron microscope. The SEM images of PLGA and pSiNP/PLGA hybrid nanofibers were collected at a beam accelerating voltage of 3 kV, InLens secondary electron detector, working distance 3-4 mm, and an aperture of 30 μm. SEM images and image analysis software were used to determine the nanofiber diameter and alignment. For this diameter and alignment, 30 nanofibers in 3 different images (90 fibers total) were quantified using NIH ImageJ software (NIH). The angles of each fiber were subtracted from the median angle of fiber alignment, and put into 15° bins.

High-magnification images and mechanical property measurements were obtained using atomic force microscopy (Asylum Research MFP-3D-Bio, Oxford Instruments, Goleta, CA). Immediately prior to measuring, samples were each individually secured to a plastic petri dish and submerged in deionized water. All images and measurements were acquired within an hour of being submerged to ensure comparable hydration states between samples, as well as to limit further sample degradation. A pyramidal, silicon nitride AFM cantilever tip (Veeco MLCT, Non-Conductive Silicon Nitride, Cantilever C, Nominal k = .01 N/m) was used in contact mode to image all samples. Once a high resolution image was obtained, the same area would then be nanoindented using force mapping mode to obtain the mechanical properties. In this mode, the cantilever is raster scanned over the sample, periodically nanoindenting the sample to acquire at least a 12 by 12 grid of indentations for a total of at least 144 indentations regardless of original image scale size (which varied with each image taken). Following experimentation, images were post processed using the MFP-3D AFM system software based in Igor Pro. Flattening order 0 and 1 and/or XY plane fitting were used to correct AFM images. For the force maps, the Hertz model was applied to each indentation point to obtain the Young's Modulus of Elasticity for each point in the force map. By cross-referencing the AFM contact mode image with the AFM force map height data, sample areas where the biomaterial has been

directly indented can by preselected prior to analysis to exclude points where the glass underneath the sample was indented instead of the sample.

Hydrodynamic size and zeta potential were measured by dynamic light scattering (DLS) using a Zetasizer ZS90 (Malvern Instruments). Water contact angles were measured using a Ramé-Hart DROPimage CA v2.5 instrument and the manufacturer's software. An Ocean Optics QE-Pro spectrometer was used to obtain steady-state photoluminescence spectra with a λ_{ex} = 365 nm LED excitation source (LLS-365, Ocean optics, USA) connected to a band pass filter (370 ±36 nm) and a 500 nm long-pass emission filter. For gated luminescence imaging of silicon nanoparticles (GLISiN),[10] the same LED source (λ_{ex}: 365 nm) was used but it was pulsed at a repetition rate of 10 Hz, externally synchronized and triggered by a function generator (Keithley3390 50 MHz arbitrary waveform generator). Time-resolved images were obtained with an intensified CCD camera (iSTAR 334T, Andor Technology Ltd.) fitted with a Nikon AF micro lens (Nikko 105 mm). Andor Solis software was used to program delays and timing pulses and to analyze images including signal-to-noise ratio (SNR). For GLISiN, a time delay of 5 μs was used and the signal was collected for 150 μs. This signal was corrected for background and then accumulated 10 times for 3 sec. SNR was calculated from the relationship:

$$SNR = \frac{Mean_{sig} - Mean_{bg}}{\sigma_{bg}}$$

where $Mean_{sig}$ is the mean integrated value of intensity measured in the ROI defined for the signal; $Mean_{bg}$ is the mean integrated value of intensity measured in the ROI defined for the background; and σ_{bg} is the standard deviation of the mean of the background signal.

bpV(HOpic) Release: bpV(HOpic) release from bpV(HOpic)-pSiNP containing hybrid nanofibers was measured as follows: 5 mg hybrid nanofibers were suspended in 1 mL PBS at

37 °C. The PBS supernatants were collected and replaced every 48 h for the duration of the experiment (10 days). UV-vis absorbance at λ = 305nm was used to determine the concentration of bpV(HOpic) at each time point.

TrkB Aptamer Release: TrkB aptamer release from TrkB aptamer-pSiNP containing hybrid nanofibers was measured as follows: 5 mg hybrid nanofibers were suspended in 1 mL PBS at 37 °C. The PBS supernatants were collected and replaced every 48 h for the duration of the experiment (20 days). RNA release was determined by measuring the supernatants at each timepoint using a NanoDrop 2000 spectrometer.

NGF Release: NGF release from NGF-pSiNP containing hybrid nanofibers was measured as follows: 5 mg hybrid nanofibers were suspended in 1 mL PBS at 37 °C. The PBS supernatants were collected and replaced every 48 h for the duration of the experiment (42 days). The amount of NGF released was determined using a Human beta-NGF DuoSet ELISA according to the manufacturers' protocol.

Dorsal root ganglia (DRG) isolation and culture - All animal work was performed with prior approval and in accordance with the Animal Care and use Committee guidelines at the University of Michigan. Primary DRG comprised of sensory neurons and Schwann cells were isolated from post-natal day 2 C57BL/6J mouse pups (Jackson Labs, Bar Harbor, ME, USA). The DRG were cleaned of additional tracts protruding from the spheroid structure. Prior to seeding, PLGA films, nanofibers, and nanofiber hybrids were disinfected with 70% ethanol for 60 seconds and then rinsed with sterile Hank's Balanced Salt Solution (HBSS; Gibco). HBSS was removed and substrates were coated with 5 μg mL^{-1} laminin (Gibco) and incubated at room temperature for 1 hr. Substrates were rinsed with HBSS to remove excess laminin.

The DRG were seeded directly on the prepared films and fibers. They were allowed to attach for 5 min, at which point 10 μL of Neurobasal Media (Gibco) was added to prevent the cells from drying out. Each DRG was allowed an additional 15 min to adhere to the substrate, after which the substrate and DRG were covered with culture media comprised of Neurobasal Media supplemented with 1X B27 (Gibco), 1X N2 (Gibco), and 50 U/mL penicillin/streptomycin (Gibco). DRG were cultured on the PLGA substrates for 7 days with culture media replaced every 2 days.

Immunocytochemistry Analysis – DRG were chemically fixed with 4% paraformaldehyde (Sigma, St. Louis, MO, USA) for 10 min, after which they were rinsed in HBSS. Samples were permeabilized with 0.1% Triton-X in HBSS (Sigma) for 10 min and then blocked with 10% goat serum for 1 hour. Rabbit anti-Neurofilament-200 (NF-200; Sigma) with a goat anti-rabbit IgG Alexafluor555 (Life Technologies, Carlsbad, CA, USA) secondary antibody was used to visualize neurite extension from the DRG. Nuclei were stained with Hoechst 33342 (Life Technologies) and used to assess glial cell migration. Immunostained samples were imaged in fluorescence and phase contrast using an Axio Observer inverted fluorescence microscope (Zeiss, Oberkochen, Germany) using both 5X and 10X dry objectives. Immunostained images were analyzed for neurite outgrowth (length, directionality) and glial cell migration (distance, nuclei orientation) using ImageJ software (NIH, Bethesda, MD, USA). The NeuriteJ plugin for ImageJ was used to assess neurite outgrowth length by automatically quantifying the number of intersections along circles radiating from the DRG body outward in 50 μm intervals.[11] The number of intersections (e.g. neurites) was graphed by distance from the DRG body based on this data. Additionally, the longest 10 neurites were identified from this dataset. Neurite alignment was measured from the DRG body to the tip of the neurite for a minimum of 20 neurites with the exception of some of the DRG on film which had fewer than 20 neurites. For alignment analysis values between 0-90 were provided

with 0 indicating perfect alignment with the orientation of the fibers and 90 indicated neurites perpendicular to the direction of the fibers. All nuclei outside of the body of the DRG were quantified for distance from the DRG centroid to obtain migration distance and for angle of the longest axis, indicating alignment relative to the axis of alignment with the fibers.[12] For these data we interpret nuclei as non-neuronal cell migration based on their size and negative immunoreactivity with the neuron-specific markers. All data are presented as the mean +/- standard error with n =5.

Statistical Analysis: All data in this article were expressed as the mean ± standard error. Multiple comparison pairs were analyzed using a one-way or two-way ANOVA with Tukey post-hoc test in the case of longest neurite or migration distance (one-way) or alignment angle (two-way). Significance was defined at a level of $p < 0.05$. For an assessment of neurite intersections or Schwann cell migration range, a non-parametric one-way ANOVA with Dunn's post-hoc test, also known as a Friedman test, was used to assess the signficance in neurite or cell density over distance.

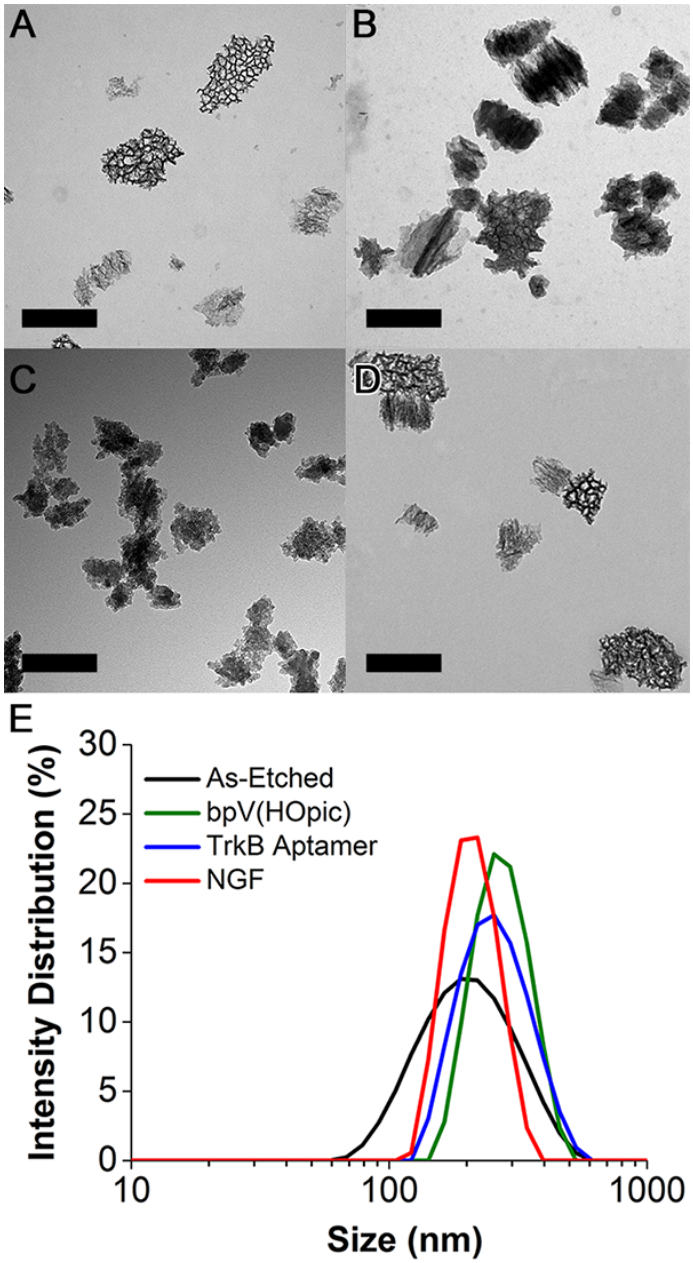

Supplemental Figure S1: TEM images of (A) as-etched pSiNPs, (B) bpV(HOpic)-loaded pSiNPs, (C) TrkB aptamer-loaded pSiNPs, (D) and NGF-loaded pSiNPs. Scale bars = 200 nm. (E) Size distribution of the different pSiNP formulations measured by dynamic light scattering (DLS).

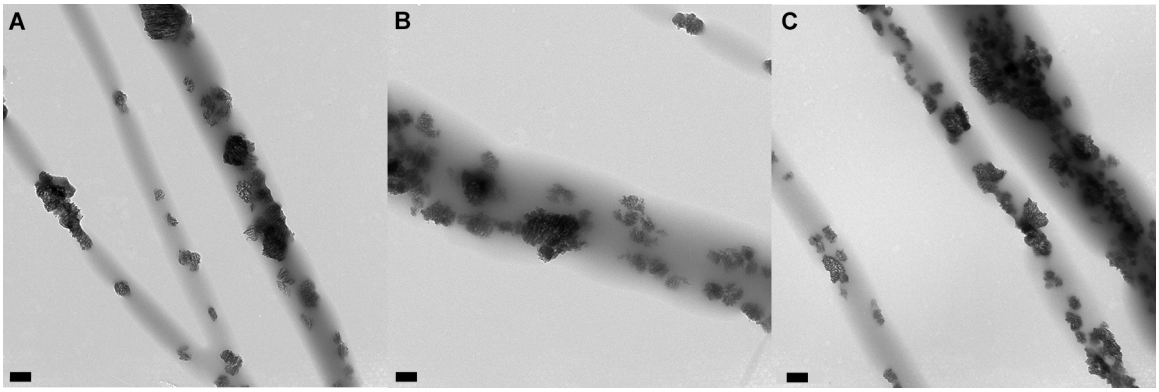

Supplemental Figure S2: TEM images of (A) bpV(HOpic)-loaded pSiNP nanofibers, (B) TrkB aptamer-loaded pSiNP nanofibers, (C) and NGF-loaded pSiNP nanofibers. Scale bars = 200 nm.

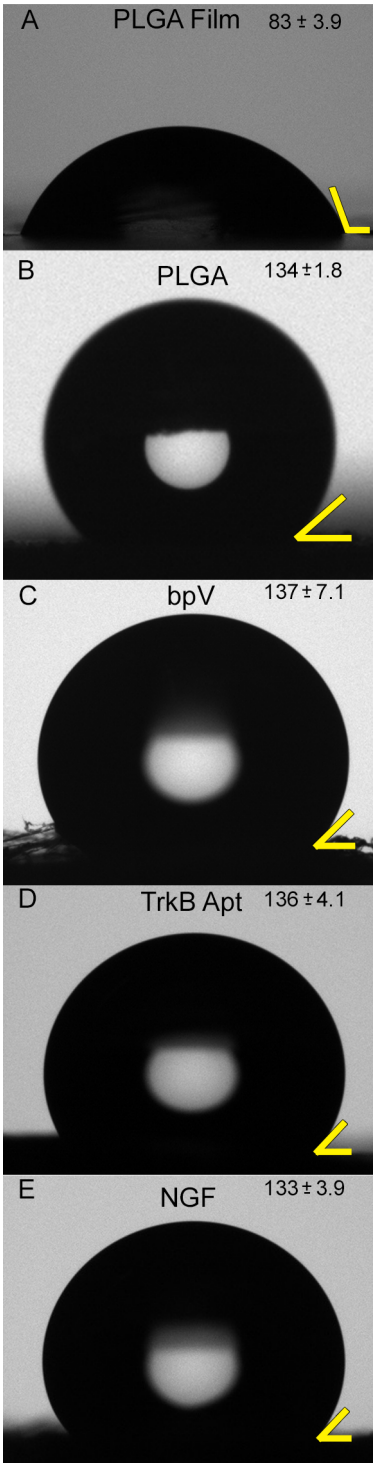

Supplemental Figure S3. Water contact angles and images measured on scaffolds of PLGA nanofibers: (A) PLGA film control, (B) PLGA nanofiber control (C) bpV(HOpic)-loaded pSiNP/PLGA hybrid nanofibers, (D) TrkB aptamer-loaded pSiNP/PLGA hybrid nanofibers, and (E) NGF-loaded pSiNP/PLGA hybrid nanofibers.

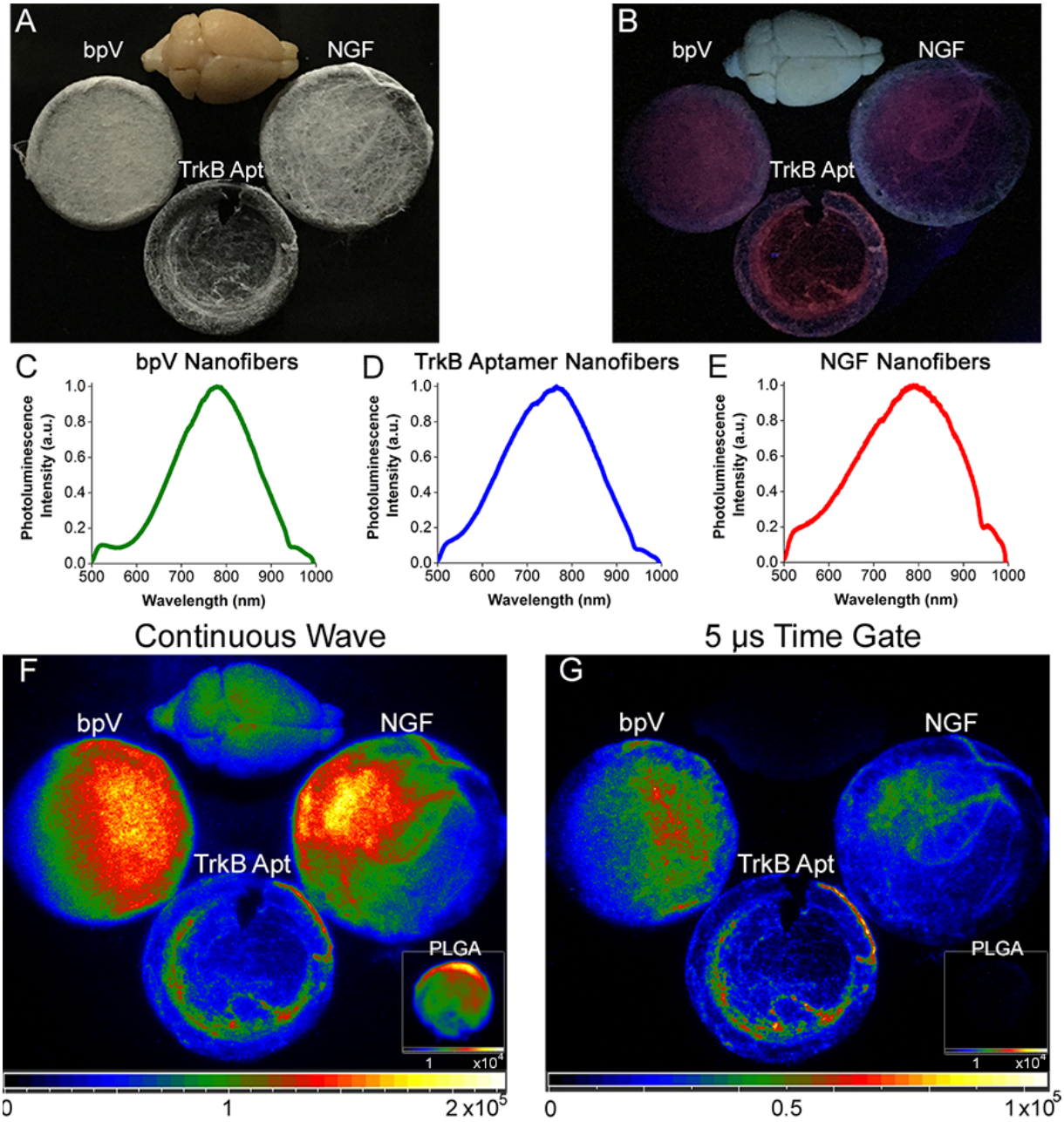

Supplemental Figure S4. Steady-state and time-gated photoluminescence images of hybrid nanofiber scaffolds. Image of a fixed mouse brain (top) bpV(HOpic)-loaded pSiNP/PLGA hybrid nanofibers (left) TrkB aptamer-loaded pSiNP/PLGA hybrid nanofibers (bottom), and NGF-loaded pSiNP/PLGA hybrid nanofibers (right) imaged under (A) ambient light or (B) excited with continuous λ_{ex} = 365 nm light emitting diode (LED). Photoluminescence emission spectra of (C) bpV(HOpic)-loaded pSiNP/PLGA hybrid nanofibers, (D) TrkB aptamer-loaded pSiNP/PLGA hybrid nanofibers, and (E) NGF-loaded pSiNP/PLGA hybrid nanofibers. Time-gated images were captured using a 5 µs excitation-acquisition delay gate. Time gating removes the prompt emission and scattered light from the image. Because the fixed mouse brain has no long-lived photoluminescence, the time-gated image of this tissue appears black. Photoluminescence images (λ_{ex} = 365 nm) were captured using a macro lens fitted to the intensified CCD camera in order to survey under (F) continuous wave excitation or under (G) a 5 µs excitation-acquisition delay gate.

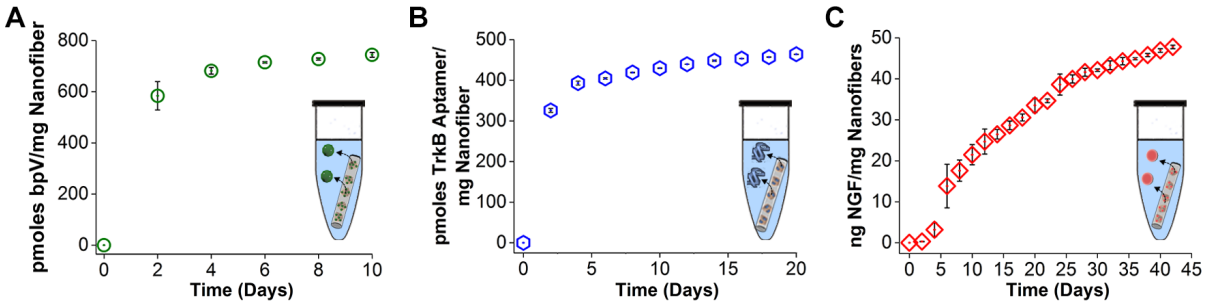

Supplemental Figure S5. Release of therapeutics from the hybrid nanofibers as a function of time in PBS buffer at 37 °C. (A) bpV(HOpic) shows a burst release over the first 2 days, and then slowly releases for the subsequent 8 days. (B) TrkB aptamer displays a burst release over the first 2 days, release slows between days 2-4, and then the material displays a relatively slow, linear release for the next 16 days. (C) NGF shows a relatively steady release for 40 days, with no initial burst.

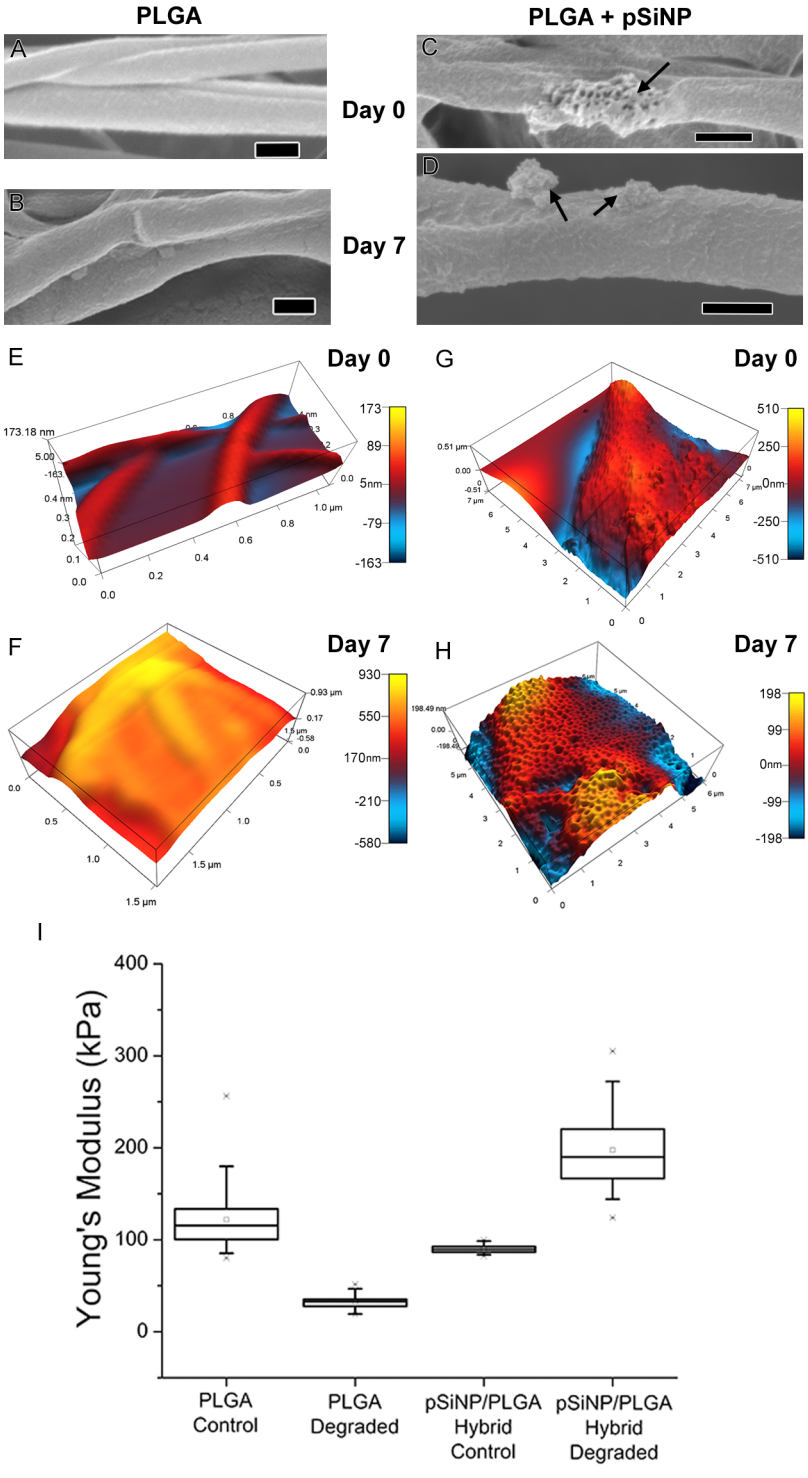

Supplemental Figure S6. Nanofiber imaging following 7 days in PBS @ 37 °C. SEM images of PLGA nanofiber controls at day 0 (A) and day 7 (B) and pSiNP/PLGA nanofibers at day 0 (C) and day 7 (D) in PBS at 37 °C. The timeline was chosen to mimic the dorsal root ganglion culture experiments. pSiNP nanoparticles (arrows) on the fiber surface display their typical porous structure prior to degradation (C). Following 7 days in PBS at 37 °C, the pSiNPs visibly degrade and lose their porous structure (D). In PLGA controls, nanofibers were relatively smooth at day 0 (E) and day 7 (F) in PBS at 37 °C. In pSiNP/PLGA samples, nanofibers displayed surface indentations between 10-40 nm at day 0 (G) and day 7 (H) in PBS at 37 °C. While pSiNP degradation is obvious in the SEM images, nanofiber surface indentations seem to be due to fabrication and not surface changes due to incubation in PBS at at 37 °C for 7 days. Young's modulus values were obtained using AFM nanoindenting force mapping (I). Young's modulus of PLGA control nanofibers saw a reduction from 122 ±33 to 32 ±8 kPA following 7 days incubation. Young's modulus of pSiNP/PLGA nanofibers saw an increase in Young's modulus values from 90 ±4 to 198 ±41 kPa following 7 days incubation, potentially due to increased AFM cantilever contact with nanoparticles as pSiNPs degrade and shed their PLGA surface coatings.

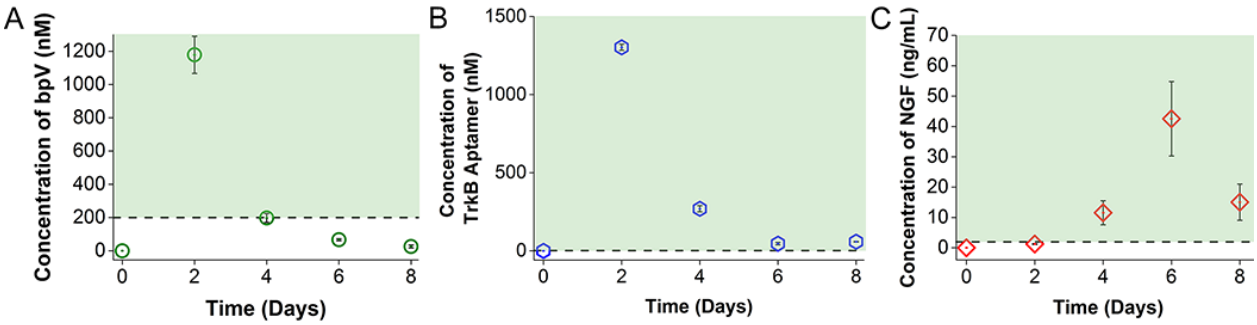

Supplemental Figure S7. The predicted concentrations of (A) bpV(HOpic), (B) TrkB aptamer, and (C) NGF during culture of DRG explants as a function of time *in vitro*. The dashed line signifies the minimum concentration of API necessary to evoke a neuronal response, based on literature reports. Predictions are based on the release data for the three therapeutics, determined from separate *in vitro* (PBS, 37 °C) measurements (Supplemental Figure S5), and assume 2 mg of hybrid nanofibers in 500 µL of cell culture media. The small molecule bpV(HOpic) released from hybrid nanofibers is above this minimum concentration between day 2 and day 4, TrkB aptamer is above the minimum concentration for all the culture time points, and NGF is at or above the minimum concentration between day 2 and day 8.

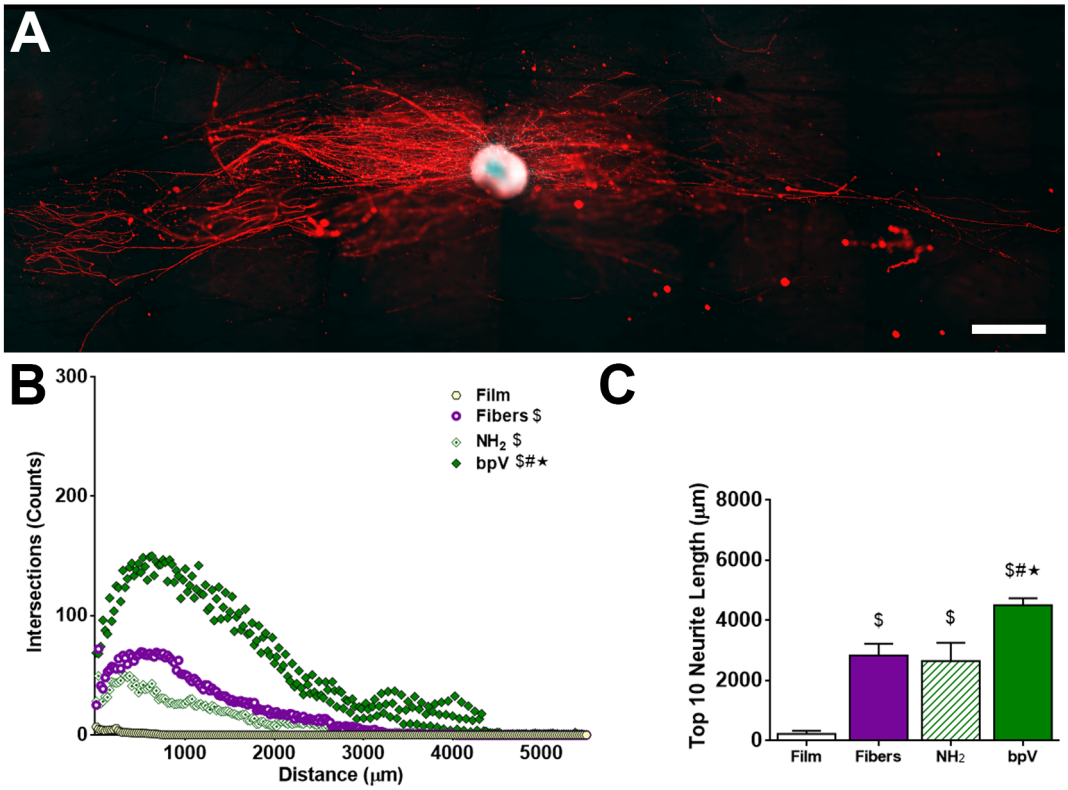

Supplemental Figure S8. Control experiments for the tests of efficacy of bpV(HOpic)-pSiNP/PLGA on DRG explant neurite extension (Fig. 4 of the main text). The control nanofibers for these experiments ("NH_2") contain the same amine surface chemistry as the bpV(HOpic)-pSiNP/PLGA nanofibers, except the pSiNPs were not loaded with bpV(HOpic). (A) NF200 stained DRG cultured on the "NH_2" control nanofibers (amine-functionalized-pSiNP/PLGA), obtained after 7 days of growth. (B) Neurite extension range, comparing the "NH_2" nanofiber control, a pure PLGA film control ("Film"), and a pure PLGA nanofiber control ("Fiber") with the bpV(HOpic)-pSiNP/PLGA sample. (C) Average length of the top 10 (longest) neurites from DRGs, comparing "NH_2" nanofiber control, a pure PLGA film control ("Film"), and a pure PLGA nanofiber control ("Fiber") with bpV(HOpic)-loaded pSiNP/PLGA hybrid nanofibers. The bpV(HOpic)-loaded pSiNP/PLGA hybrid nanofibers induce significantly more robust neurite extension and longer outgrowth of neurites compared to controls. Scale bar = 500 μm. n=5 all groups $= $p<0.05$ compared to PLGA films. #= $p<0.05$ compared to PLGA fibers. *= $p<0.05$ compared to amine-functionalized-pSiNP/PLGA nanofibers.

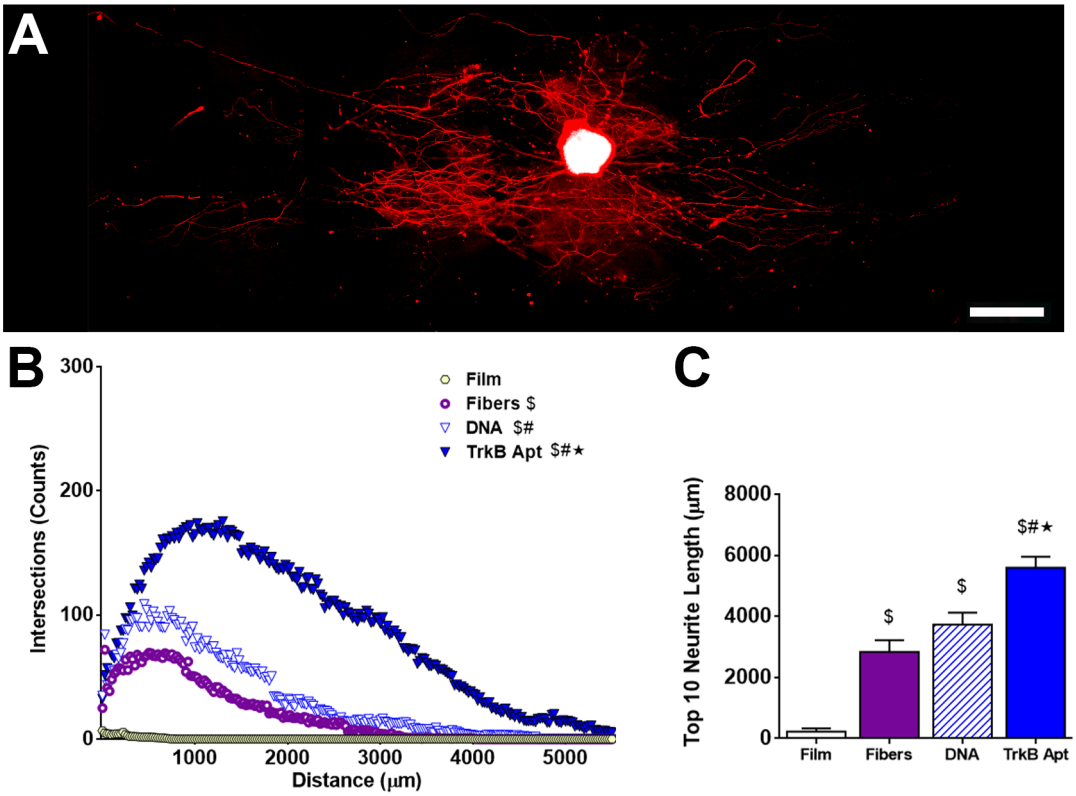

Supplemental Figure S9. Control experiments for the tests of efficacy of TrkB aptamer-pSiNP nanofiber hybrids on DRG explant neurite extension (Fig. 4 of the main text). The control nanofibers for these experiments ("DNA") contain a sham DNA strand in place of the aptamer, and the same calcium silicate sealing chemistry was used to load the DNA into the pSiNPs as was used with the aptamer. (A) NF200 stained DRG cell cultured on DNA-pSiNP/PLGA control nanofibers, obtained after 7 days of growth. (B) Neurite extension range, comparing the "DNA" nanofiber control, a pure PLGA film control ("Film"), and a pure PLGA nanofiber control ("Fiber") with the TrkB aptamer-pSiNP nanofiber hybrids. (C) Average length of the top 10 (longest) neurites from DRGs, comparing "DNA" nanofiber control, a pure PLGA film control ("Film"), and a pure PLGA nanofiber control ("Fiber") with TrkB aptamer-loaded pSiNP nanofiber hybrids. The TrkB aptamer-pSiNP/PLGA hybrid nanofibers induce significantly more robust neurite extension and longer outgrowth of neurites compared with pure PLGA film, pure PLGA nanofiber, and DNA-pSiNP/PLGA nanofiber controls. Scale bar = 500 μm. n=5 all groups $= $p<0.05$ compared to PLGA films. #= $p<0.05$ compared to PLGA fibers. *= $p<0.05$ compared to DNA-pSiNP/PLGA nanofibers.

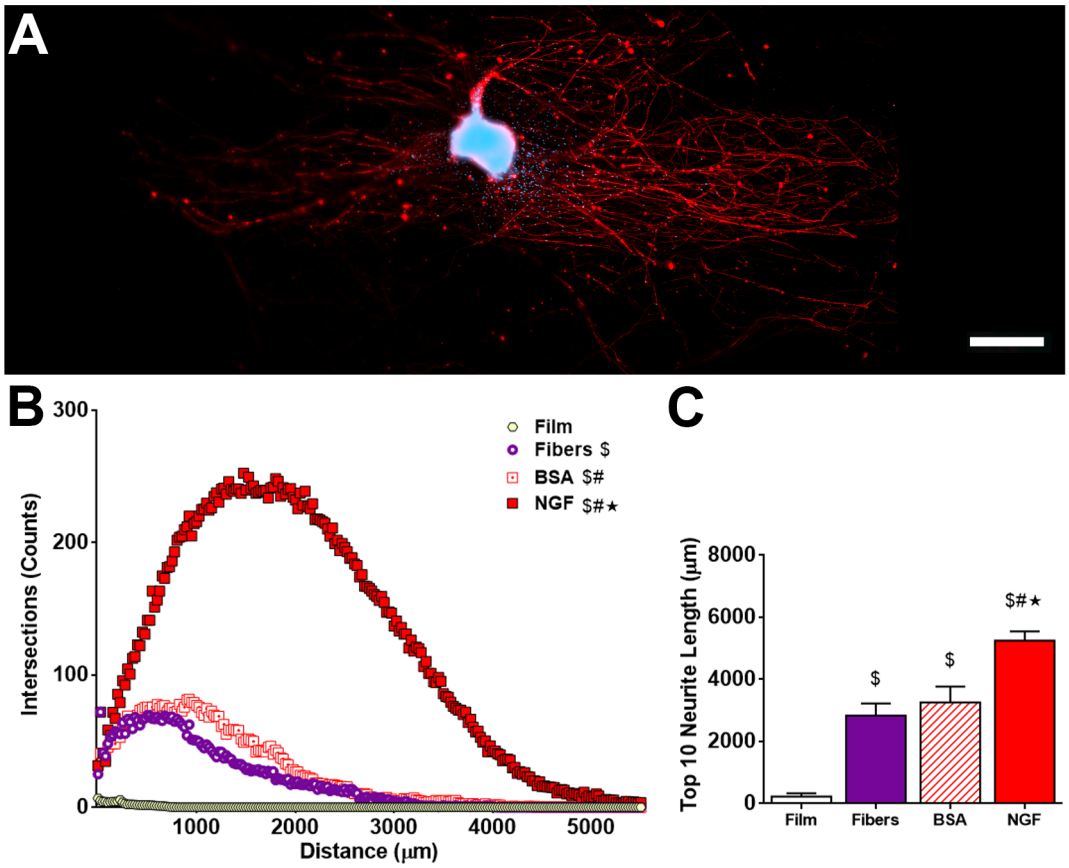

Supplemental Figure S10. Control experiments for the tests of efficacy of NGF-pSiNP nanofiber hybrids on DRG explant neurite extension (Fig. 4 of the main text). The control nanofibers for these experiments ("BSA") contain bovine serum albumin as a sham protein in place of NGF, and the same oxidative trapping chemistry was used to load BSA into the pSiNPs as was used with the NGF protein. (A) NF200 stained DRG cell cultured on BSA-pSiNP/PLGA control nanofibers. (B) Neurite extension range, comparing the "BSA" nanofiber control, a pure PLGA film control ("Film"), and a pure PLGA nanofiber control ("Fiber") with the NGF-pSiNP nanofiber hybrids. (C) Average length of the top 10 (longest) neurites from DRGs, comparing "BSA" nanofiber control, a pure PLGA film control ("Film"), and a pure PLGA nanofiber control ("Fiber") with NGF-loaded pSiNP nanofiber hybrids. The NGF-pSiNP/PLGA hybrid nanofibers induce significantly more robust neurite extension and longer outgrowth of neurites compared with pure PLGA film, pure PLGA nanofiber, and BSA-pSiNP/PLGA nanofiber controls. Scale bar = 500 μm. n=5 all groups $= $p<0.05$ compared to PLGA films. #= $p<0.05$ compared to PLGA fibers. *= $p<0.05$ compared to BSA-pSiNP/PLGA nanofibers.

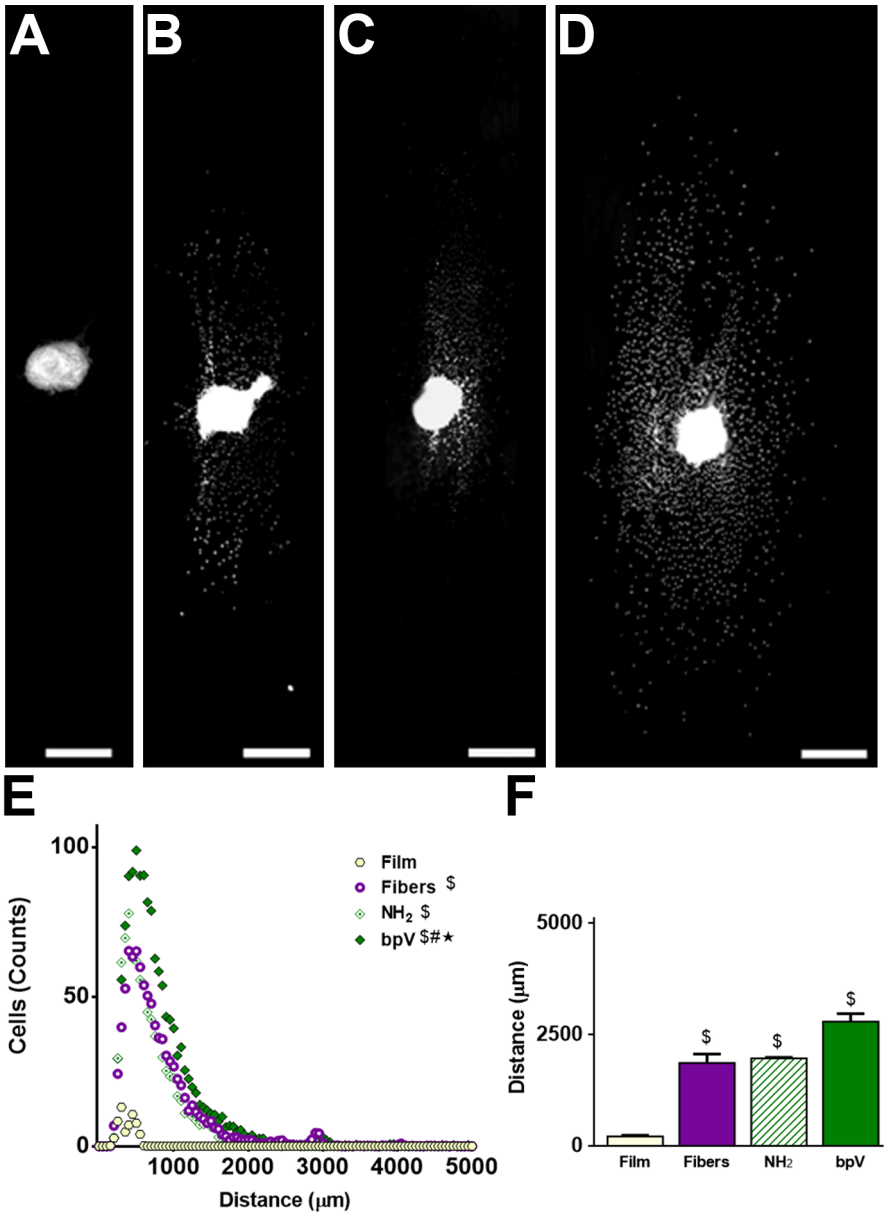

Supplemental Figure S11. Control experiments for the tests of efficacy of bpV(HOpic)-pSiNP nanofiber hybrids on DRG explant cellular migration (Fig. 5 of the main text). Control samples as described in Supplemental Fig. S7. Hoechst stained nuclei from DRG explants seeded on (A) PLGA films, (B) PLGA nanofibers, (C) amine-functionalized pSiNP/PLGA nanofibers, and (D) bpV(HOpic)-pSiNP/PLGA hybrid nanofibers. (E) Range comparisons showing that more cells migrated from the DRG explant on bpV(HOpic)-pSiNP/PLGA hybrid nanofibers compared to the three control scaffolds. (F) The average of the ten longest migrating cells on bpV(HOpic)-pSiNP/PLGA hybrid nanofibers only showed a significant increase compared to PLGA film controls. No significant differences in cell migration were seen between the three nanofiber groups. Scale bar = 500 μm. n=5 all groups $= $p<0.05$ compared to PLGA films. #= $p<0.05$ compared to PLGA fibers. *= $p<0.05$ compared to amine-functionalized-pSiNP/PLGA nanofibers.

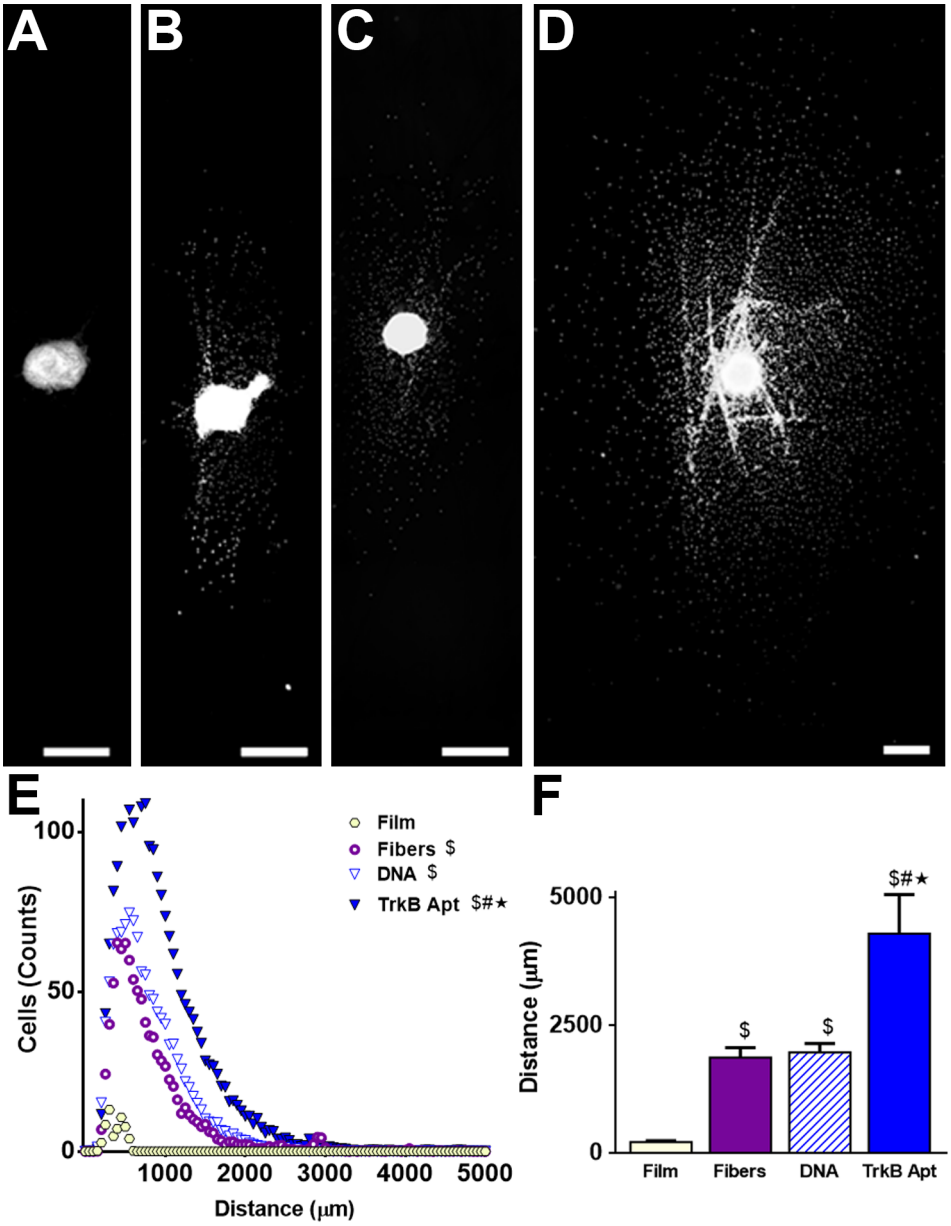

Supplemental Figure S12. Control experiments for the tests of efficacy of TrkB aptamer-pSiNP nanofiber hybrids on DRG explant cellular migration (Fig. 5 of the main text). Control samples as described in Supplemental Fig. S8. Hoechst stained nuclei from DRG explants seeded on (A) PLGA films, (B) PLGA nanofibers, (C) DNA-pSiNP/PLGA nanofibers, and (D) TrkB aptamer-pSiNP/PLGA hybrid nanofibers. (E) Range comparisons show that more cells migrated from the DRG explant on TrkB aptamer-pSiNP/PLGA hybrid nanofibers compared to the three control scaffolds. (F) Average of the ten longest migrating cells on TrkB aptamer-pSiNP/PLGA hybrid nanofibers show significantly greater cell migration compared to the three control scaffolds. Scale bar = 500 μm. n=5 all groups $= $p<0.05$ compared to PLGA films. #= $p<0.05$ compared to PLGA fibers. *= $p<0.05$ compared to DNA-pSiNP/PLGA nanofibers.

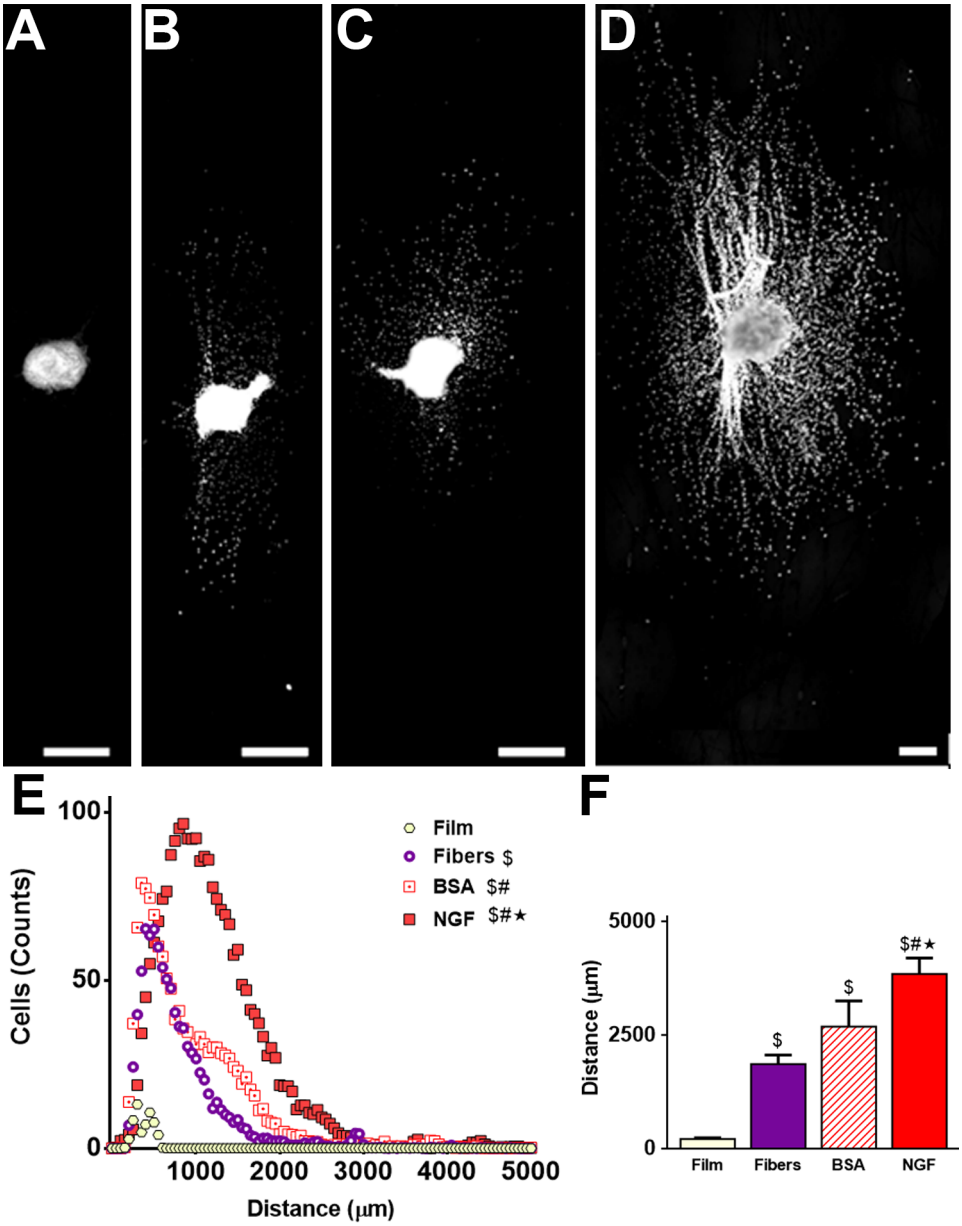

Supplemental Figure S13. Control experiments for the tests of efficacy of NGF-pSiNP nanofiber hybrids on DRG explant cellular migration (Fig. 5 of the main text). Control samples as described in Supplemental Fig. S9. Hoechst stained nuclei from DRG explants seeded on (A) PLGA films, (B) PLGA nanofibers, (C) BSA-pSiNP/PLGA nanofibers, and (D) NGF-pSiNP/PLGA hybrid nanofibers. (E) Range comparisons show that more cells migrated from the DRG explant on NGF-pSiNP/PLGA hybrid nanofibers compared to the three control scaffolds. (F) Average of the ten longest migrating cells on NGF-pSiNP/PLGA hybrid nanofibers show significantly greater cell migration compared to the three control scaffolds. Scale bar = 500 μm. n=5 all groups $= $p<0.05$ compared to PLGA films. #= $p<0.05$ compared to PLGA fibers. *= $p<0.05$ compared to BSA-pSiNP/PLGA nanofibers.

Dynamic Light Scattering		
Particle Type	**Mean Diameter (nm)**	**Zeta Potential (mV)**
As-Etched	187 ±3.2	-45 ±1.5
Amine Functionalized	243 ±1.5	35 ±5.5
DNA Control	248 ±3.2	4.1 ±0.7
BSA Control	211 ±3.2	-29 ±5.7
bpV(HOpic)	262 ±1.1	4.4 ±2.2
TrkB Aptamer	257 ±2.5	3.7 ±0.4
NGF	206 ±2.1	-24 ±4.3

Supplemental Table S1: Hydrodynamic diameter (z-average) and zeta potential measured on as-etched porous silicon nanoparticles (pSiNPs) and the pSiNP products of amine functionalization, bpV(HOpic) loading, TrkB aptamer loading, and NGF loading. The size and zeta potential values were measured in DI H_2O. The standard deviations are calculated from 3 replicate measurements. PDI values were all < 0.2.

Signal-to-Noise Ratio Analysis		
Sample Type	**No Time Gate**	**5 µs Time Gate**
Brain	101 ±2.4	5 ±1.1
PLGA	156 ±10.9	6 ±4.3
bpV(HOpic)	144 ±27.7	229 ±40.1
TrkB Aptamer	184 ±24.5	172 ±35.1
NGF	131 ±39.9	147 ±46.1

Supplementary Table S2. Signal-to-noise ratio (SNR) analysis of steady-state and time-gated photoluminescence imaging data. SNR of survey images of fixed mouse brain tissue, bpV(HOpic)-pSiNP PLGA nanofibers, TrkB aptamer-pSiNP PLGA nanofibers, and NGF-pSiNP PLGA nanofibers (n=3 ROI in each image).

References:

[1] Z. Qin, J. Joo, L. Gu, M. J. Sailor, *Part. Part. Syst. Charact.* **2014**, 31, 252.

[2] J. M. Zuidema, T. Kumeria, D. Kim, J. Kang, J. Wang, G. Hollett, X. Zhang, D. S. Roberts, N. Chan, C. Dowling, E. Blanco-Suarez, N. J. Allen, M. H. Tuszynski, M. J. Sailor, *Advanced Materials* **2018**, 30.

[3] J. Joo, J. F. Cruz, S. Vijayakumar, J. Grondek, M. J. Sailor, *Adv. Funct. Mater.* **2014**, 24, 5688.

[4] D. Kim, J. M. Zuidema, J. Kang, Y. Pan, L. Wu, D. Warther, B. Arkles, M. J. Sailor, *Journal of the American Chemical Society* **2016**, 138, 15106.

[5] M. S. Kim, A. El-Fiqi, J. W. Kim, H. S. Ahn, H. Kim, Y. J. Son, H. W. Kim, J. K. Hyun, *ACS Appl. Mater. Interfaces* **2016**, 8, 18741.

[6] Y. Z. Huang, F. J. Hernandez, B. Gu, K. R. Stockdale, K. Nanapaneni, T. E. Scheetz, M. A. Behlke, A. S. Peek, T. Bair, P. H. Giangrande, J. O. McNamara, *Molecular Pharmacology* **2012**, 82, 623.

[7] A. Judefeind, M. M. de Villiers, *Drug Loading into and in vitro release from nanosized drug delivery systems*, Springer Science & Business Media, New York, NY **2008**.

[8] J. M. Zuidema, T. Kumeria, D. Kim, J. Y. Kang, J. A. N. Wang, G. Hollett, X. Zhang, D. S. Roberts, N. Chan, C. Dowling, E. Blanco-Suarez, N. J. Allen, M. H. Tuszynski, M. J. Sailor, *Advanced Materials* **2018**, 30.

[9] E. Segal, L. A. Perelman, F. Cunin, F. Di Renzo, J. M. Devoisselle, Y. Y. Li, M. J. Sailor, *Adv Funct Mater* **2007**, 17, 1153.

[10] J. Joo, X. Liu, V. R. Kotamraju, E. Ruoslahti, Y. Nam, M. J. Sailor, *ACS Nano* **2015**, 9, 6233.

[11] A. Torres-Espin, D. Santos, F. Gonzalez-Perez, J. del Valle, X. Navarro, *J Neurosci Methods* **2014**, 236, 26.

[12] J. M. Zuidema, M. C. Hyzinski-Garcia, K. Van Vlasselaer, N. W. Zaccor, G. E. Plopper, A. A. Mongin, R. J. Gilbert, *Biomaterials* **2014**, 35, 1439.